Research Article

Numerical Modeling for Corrosion Rate between Heat-affected Zone and Unaffected Base Metal of Galvanized Steel Welded by Brazing

Adisak Pinyo
Department of Materials Engineering, Faculty of Engineering, Kasetsart University, Bangkok, Thailand

Sompong Bangyeekhan
Department of Teacher Training in Mechanical Engineering, Faculty of Technical Education, King Mongkut's University of Technology North Bangkok, Bangkok, Thailand

Trinet Yingsamphancharoen*
Center of Welding Engineering and Metallurgical Inspection, Science and Technology Research Institute, King Mongkut's University of Technology North Bangkok, Bangkok, Thailand
Department of Welding Engineering Technology, College of Industrial Technology, King Mongkut's University of Technology North Bangkok, Bangkok, Thailand

Aphichart Rodchanarowan*
Department of Materials Engineering, Faculty of Engineering, Kasetsart University, Bangkok, Thailand

* Corresponding author. E-mail: trinet.y@cit.kmutnb.ac.th, fengacrw@ku.ac.th DOI: 10.14416/j.asep.2021.03.001
Received: 16 November 2020; Revised: 8 January 2021; Accepted: 18 January 2021; Published online: 1 March 2021

Abstract
Brazing of galvanized steel causes decaying of the zinc coating and decreasing of corrosion resistance on heat-affected zone (HAZ) and weldment. The corrosion rates among the HAZ, unaffected base metal (UBM), and weldment of galvanized steel welded by brazing were numerically modeled by COMSOL Multiphysics. The numerically modeled current density values from various zones, such as the couples between the HAZ and the UBM, between the weldment and the HAZ, and between the UBM and steel were used to calculate the corrosion rates. In this work, two different methods based on Faraday's Law, the mixed potential theory and the Numerical modeling, were compared for calculations of the corrosion rates of each region. Using the mixed potential theory, the calculated corrosion rates of regions I, II, III, IV, V and VI were 0.853, 0.284, 2.105,1.754, 2.028, and 0.554 mm/y, respectively. Where as based on the Numerical modeling, these rates of all regions were 0.918, 0.275, 2.198, 1.904, 2.151, and 0.566 mm/y, in orderly. These comparisons suggested that the corrosion rates obtained from the two methods were similar. However, the results showed that the Numerical modeling method could predict the corrosion rate with less error.

Keywords: Corrosion, Numerical modeling, Galvanized, HAZ, Welding

1 Introduction

Brazing is the welding of two materials whereby the filler rod acts as a solder. The melting point of the filler rod is lower than that of the workpiece. The brazing of galvanized steel causes the steel to be less corrosion-resistant. The heat generated in the brazing process causes the zinc coating to decay. The heat-affected zone and weld areas are the most affected by the brazing process.

Corrosion is associated with welded structures, since the microstructure, properties, and compositions of the weld metal and HAZ are quite different than those of the base metals. the corrosion rate associated with welds is much higher than the base metals. The reason for this is usually a combination of the effect of microstructure and residual stress. Highly stressed regions surrounding welds may result in accelerated corrosion relative to the base metal [1]. In this work, we focused on galvanic corrosion. The galvanic corrosion [2] is a chemical potential difference between dissimilar metals when both types of metals have electrical contact. The potential difference results in a flow of current between the two metal objects. When two metal materials are connected electrically in a corrosive environment, corrosion occurs in the anodic material [1].

Previously, a research was conducted to monitor on zinc decay in the HAZ. The brazing of galvanized steel was conducted at currents of 70, 75, 80, 85, 90, and 95 A. When the brazing current increased, the remaining zinc on the HAZ decreased [3]. The HAZ has a corrosion rate similar to that of steel, but the zones with a large amount of zinc have higher corrosion rates [3].

Considering the importance of corrosion, a method for estimating the corrosion rate before actual corrosion is investigated in this study. This study proposes a numerical model, which is used to solve mathematical equations and to predict the corrosion current. COMSOL Multiphysics, a computer program that can simulate an environment similar to the real environment, is used in this study. COMSOL can be applied to create corrosion models that show results in terms of corrosion current density and corrosion potential [4]–[7].

In a previous study, galvanic cells between magnesium alloy (AE44) and steel and magnesium alloy and aluminum alloy (AA6063) were investigated by determining the corrosion current density obtained from the mixed potential theory, and the results were compared with numerical modeling results. When the corrosion rate was calculated, it was found that the magnesium alloy (AE44) and steel had corrosion rates of 231 and 210 mm/year, respectively, and those rates of magnesium alloy and aluminum alloy (AA6063) were similar: 26 and 29 mm/year, respectively [8].

The numerical model predicted the corrosion rate of galvanic couple by COMSOL Multiphysics. The modeling from experimental data can be predicted by this method successfully [9], [10]. The numerical model is also applied to predict the corrosion rate of weld joint. The corrosion rate from the model are compared with mixed potential theory and experimental techniques. The predicted corrosion rate using the numerical model is 10% of the estimated rate obtained from the mixed potential theory, and is 10–20% from the experiment [11].

In this study, the importance of corrosion rates caused by the potential differences in galvanized steel occurring during the brazing process was monitored and modeled by using the Numerical modeling by COMSOL Multiphysics method. Specifically, the numerically modeled current density values were obtained from the various regions of metal objects to calculate the corrosion rates. The corrosion rates obtained from the numerical modeling and the mixed potential theory were compared. The predicted corrosion rate and heat occured on galvanized steel during the brazing process could decrease damage caused by corrosion before their occurrence on the workpieces.

2 Experiment

2.1 *Materials*

Two plates of galvanized steel with dimensions of 1.2 × 160 × 120 mm were brazed at 80 A by tungsten with the Argon (Ar) gas welding using ER CuSi-A as filler. The obtained lap joint was shown in Figure 1 [3].

The welding positions were at a 45-degree angle and a 90-degree angle. Argon gas was covered under a flow rate of 20 L/min, and the welding speed was 800 mm/min. The welding distance was 110 mm. The welding process was controlled automatically. The arc voltage was stable at 2.1 V [3].

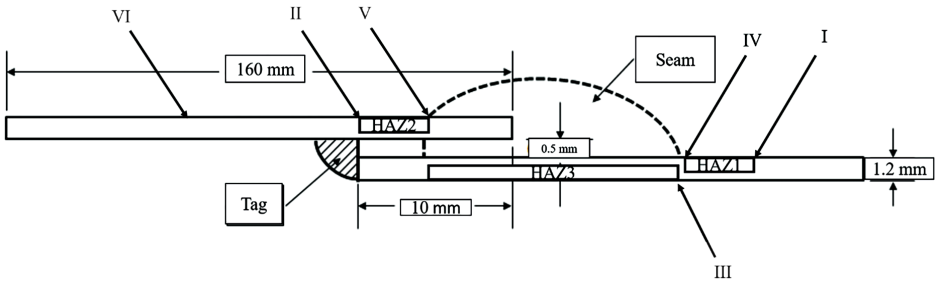

Figure 1: Brazed galvanized steel (lap joint) and region of a galvanic cell.

2.2 *Polarization experiment*

Corrosion analysis was conducted using an electrochemical test, with Pt as the counter electrode. The reference electrode was Ag/AgCl, and the working electrode was HAZ1, HAZ2, HAZ3, UBM, steel weldment in 3.5%wt NaCl. The analysis was conducted under an open circuit potential of −0.1 V to 0.1 V. The analysis rate was 0.5 mV/s [3].

2.3 *Corrosion parameter determination by the Mixed Potential theory*

The galvanic couples in the following six regions were investigated: region I HAZ1 and UBM, region II HAZ2 and UBM, region III HAZ3 and UBM, region IV weldment and HAZ1, region V weldment and HAZ2, and region VI steel and Zn. Because galvanic corrosion was caused by two different materials and potentials, therefore 6 regions have possibilities in corrosions [4], [5].

The mixed potential theory [11] was used to analyze regions I, II, III, IV, V, and VI. The corrosion current density was determined using the mixed potential theory, as shown in Figure 2. The result of the mixed potential theory was the matching of polarization graphs from the electrochemical tests of various zones of the galvanic cell. The corrosion potential and the corrosion current density of the galvanic couple were determined previously and were used in this study [4]. The polarization graph of the anode was in the zone with a lower corrosion potential than the polarization graph of the cathode. In this case, the corrosion of the galvanic couple can be predicted by the mixed potential theory. Corrosion occurred at the UBM at regions I, II, III, VI, and also at the HAZs of regions IV and V. The corrosion parameters at the intersection point of the polarization graph were shown in Table 1. The corrosion current density of galvanic couples I, II, III, IV, V, VI were shown in Table 2 [9], [10].

Table 1: Corrosion parameters in the polarization experiments

Zones	E_{corr} (V)	I_{corr} (A/m^2)	β_a (mV/ decade)	β_c (mV/ decade)
HAZ1	–0.951	0.422	79	–216
HAZ2	–0.966	0.157	30	–445
HAZ3	–0.888	0.816	57	–359
UBM	–1.011	0.037	20	–241
Weldment (WD)	–0.476	0.090	160	–378
Steel	–0.417	0.098	67	–976

2.4 *Calculation of corrosion rate from the mixed potential theory from the current density*

Prediction tools to forcast corrosion occurrences are available, however they are not suitable to predict the corrosion rate. In theory, Faraday's law can be utilized to perform this forecasting. Faraday's law is described follows Equation (1) [6]–[9], [11].

$$CR = \frac{M}{zF\rho} i \tag{1}$$

Where CR is the mass of metal lost to corrosion m/s, M is 65.409 g/mol, Faraday's constant F is 96485.34 C/mol, the atomic mass the electron number z is 2, the density ρ is 7140 kg/m^3 for the corroding elemental of the galvanic steel, and the current density is in A/m^2.

3 Model Development

3.1 *Governing equation*

Mass transfer to an electrode is governed by the Nernst-Planck Equation (2), [8]–[10] as follows.

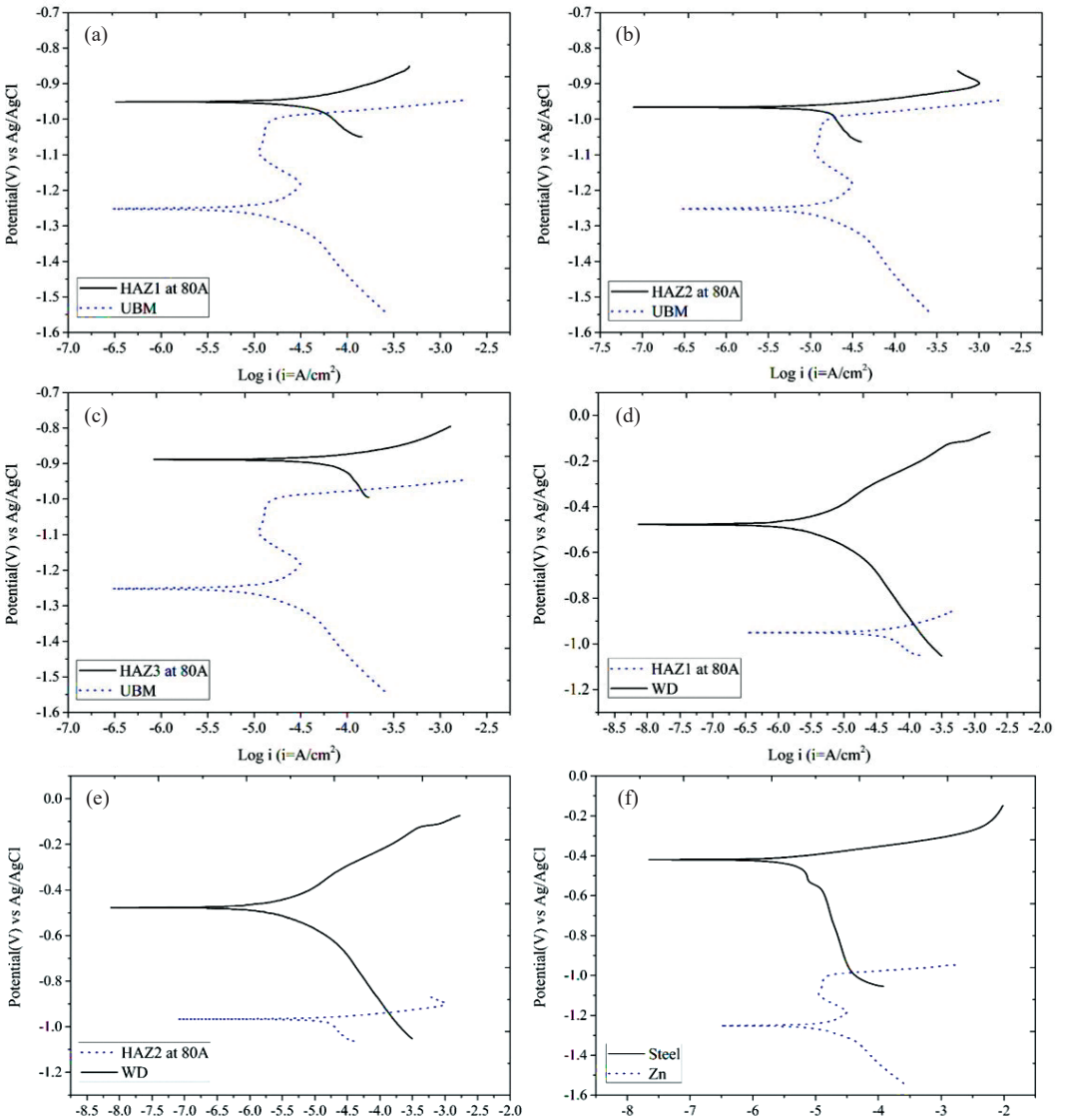

Figure 2: Polarization of various galvanic cells on the brazing of galvanized steel for the various regions considered in the mixed potential theory: (a) region I, (b) region II, (c) region III, (d) region IV, (e) region V, and (f) region VI.

$$N_i = -D\nabla c_i - z_i F u_i c_i \nabla \phi + c_i V \quad (2)$$

Where N_i is the flux of species i from the surface; mol/s.cm^2, D is the diffusion coefficient; cm^2/s, c_i is the concentration gradient, ϕ is the electric potential gradient, z_i is the charge, and u_i is the mobility of species i, F is the Faraday constant, and v is the velocity; cm/s. The three terms on the right-hand side represented the contribution of diffusion, migration, and convection, respectively, to the flux.

Equation (3) presented the conservation yields with the absence of homogeneous reactions, [8]–[11].

$$\frac{\partial c_i}{\partial t} = -\nabla \cdot N_i = D_i \nabla^2 c_i - z_i F u_i \nabla \cdot (c_i \nabla \phi) + \nabla \cdot (c_i V) \quad (3)$$

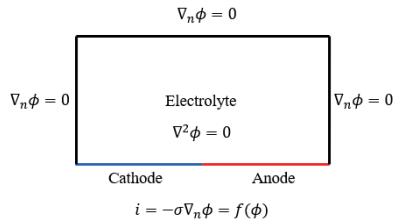

(a)

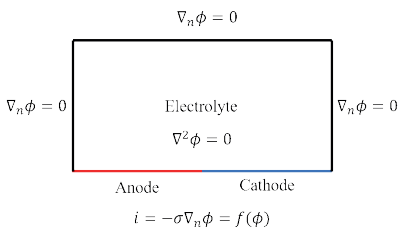

(b)

Figure 3: Governing equation and the boundary conditions.

The electrical potential in the electrolyte is governed by electrostatics described by a Poisson equation which reduces to Laplace Equation (4)

$$\nabla^2\phi = 0 \tag{4}$$

It is known that the electrolyte is continuously stimulated, so the absorption of the ion distribution is uniform though there is an equal and opposite flux of oppositely charged ions. The above equation is worked over the electrolyte domain subject to boundary conditions. The boundary conditions at the anode and the cathode surfaces are critical for predicting the corrosion rates, when mass tranfer by convection and by diffusion are neglected, as shown in Figure 3.

The polarization data obtained experimentally for dual alloys (Table 1) were used as the boundary conditions for the anode and the cathode surfaces. Both boundary conditions were given equally Equations (5) and (6) [8], [9]:

$$-\sigma\nabla_n\phi = f_a(\phi) \tag{5}$$

and,

$$-\sigma\nabla_n\phi = f_c(\phi) \tag{6}$$

Where σ the electrical conductivity of the electrolyte solution is, $f_a(\phi)$ is the current density of anodic species, $f_c(\phi)$ is the current density of cathodic species, and $\nabla_n\phi$ is a normal gradient of flux of species.

The top surface of the electrolyte can be modeled as a no-flux condition Equation (7) since air moves as an insulator. The left and right sides displayed symmetry or no-flux condition, as shown in Figure 3 [8], [9], [13].

$$\nabla_n\phi = 0 \tag{7}$$

After solving the Laplace equation subjected to the above boundary conditions, we obtained the potential and current density values at several nodes on the anode and cathode surfaces. The corrosion rate or interface speed can then be computed from the current density using Faraday's law Equation (1).

3.2 *Arbitrary Langrangian–Eulerian (ALE) method*

ALE method is an advanced moving-mesh technique with amalgamate of Eulerian and Langrangian type of extension and it can capture deformation [8]–[11].

The ALE method consists of two frames (Global and Local) for a 2D formulation with X, Y Coordinates. A global frame is a fixed frame and a local frame is moving with time. This moving was predicted through the ALE method using COMSOL Multiphysics. The geometry and boundary conditions were considered as shown in Figure 4 [14], [15].

The 2D mesh displacement was gained by solving the following Equation (8) [8]–[10]:

$$\frac{\partial^2}{\partial X^2}\frac{\partial x}{\partial t} + \frac{\partial^2}{\partial Y^2}\frac{\partial x}{\partial t} = 0 \text{ and } \frac{\partial^2}{\partial X^2}\frac{\partial y}{\partial t} + \frac{\partial^2}{\partial Y^2}\frac{\partial y}{\partial t} = 0 \tag{8}$$

The above equations indicated the smooth deformations of the mesh, considering the restraints placed on the borderline. For the cathode surface, the normal velocity was considered to be zero (no corrosion). The normal component (n) of the velocity vector (v) of the anode surface were computed using Equation (1) and represented with Equation (9) [8]–[10]:

$$n \cdot V = \frac{M}{zF\rho} i = \frac{M}{zF\rho} f_a(\phi) \tag{9}$$

The geometry and boundary conditions with the additional potential for this moving-mesh technique were shown in Figure 4.

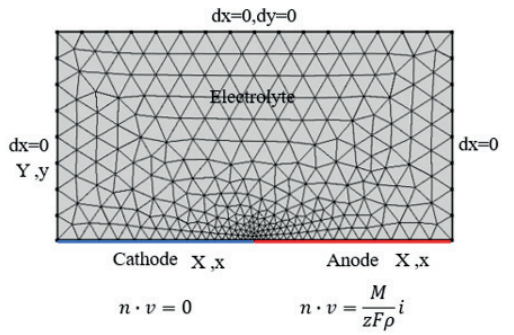

(a)

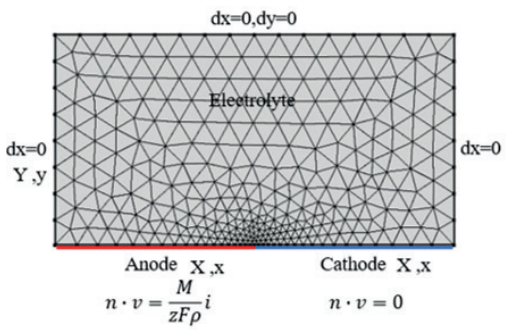

(b)

Figure 4: Boundary conditions used ALE method in COMSOL Multiphysics.

4 Results and Discussion

Each zone in this study had different parameters, which were important for the numerical modeling [8]–[10]. The results of polarization tests of HAZ1, HAZ2, HAZ3, UBM, weldment and steel were shown in Table 1.

The mixed potential theory showed that the galvanic couple between HAZ1, HAZ2, HAZ3, and the UBM corroded at the UBM because it had a lower potential than HAZ. The highest corrosion current density occurred in region III, followed by I, and then II at 1.406, 0.570, 0.190 A/m^2 respectively. It was observed that zinc decay on the surface of HAZ occurred in HAZ3<HAZ1<HAZ2 [3]. The galvanic couple between HAZ1, HAZ2, and the weldment corroded at HAZ because it had a lower potential than the weldment. The highest corrosion current density occurred in region V, followed by IV at 1.355 and 1.174 A/m^2 respectively. It was affected by zinc decay on the surface of the least amount of zinc remaining in the HAZ1<HAZ2. The galvanic couple between steel (Fe) and the surface (Zn) corroded at the surface, because the surface had lower potential than steel. The corrosion current density of this couple's reaction was 0.370 A/m^2.

Numerical modeling can define the conditions according to the governing equation using the software COMSOL Multiphysics [8]–[10]. The results provided predictions of the corrosion current density [11]. Figure 5 (left) shows the corrosion potential in the electrolyte that occured at the surface attached to the electrolyte at the red zone and it was lower than that in the blue zone. This red zone can be predicted to be a corroded anodic region. The HAZ was cathode and the surface was anodic. In regions IV and V, the weldment was cathode and HAZ was anodic. In region VI, steel was cathode, and the surface was anodic.

The corrosion current densities from the numerical modeling of regions I, II, III, IV, V, VI showed changes from the anode surface to the cathode surface (Figure 5 right) In regions I, II, III, corrosion occurred at the UBM. The highest corrosion current density occurred in region III, followed by I, and then II at 1.468, 0.610, 0.184 A/m^2 respectively. In regions IV and V, corrosion current density occurred in HAZ. The highest corrosion current density occurred in region V, followed by IV at 1.437, 1.272 A/m^2 respectively. In region VI, corrosion current density occurred at the surface was 0.378 A/m^2. The highest corrosion current density between the anodic electrode and the cathode electrode was shown in Table 2.

Table 2: Comparison of corrosion current density and corrosion rate

Regions	Corrosion Current Density (A/m^2)		Corrosion Rate (CR) in mm/y		
	Mixed Potential Theory	Numerical Modeling	Mixed Potential Theory	Numerical Modeling	%Error
I	0.570	0.610	0.853	0.913	7.01
II	0.190	0.184	0.284	0.275	3.15
III	1.406	1.468	2.105	2.198	4.40
IV	1.174	1.272	1.754	1.904	8.34
V	1.355	1.437	2.028	2.151	6.05
VI	0.370	0.378	0.554	0.566	2.16

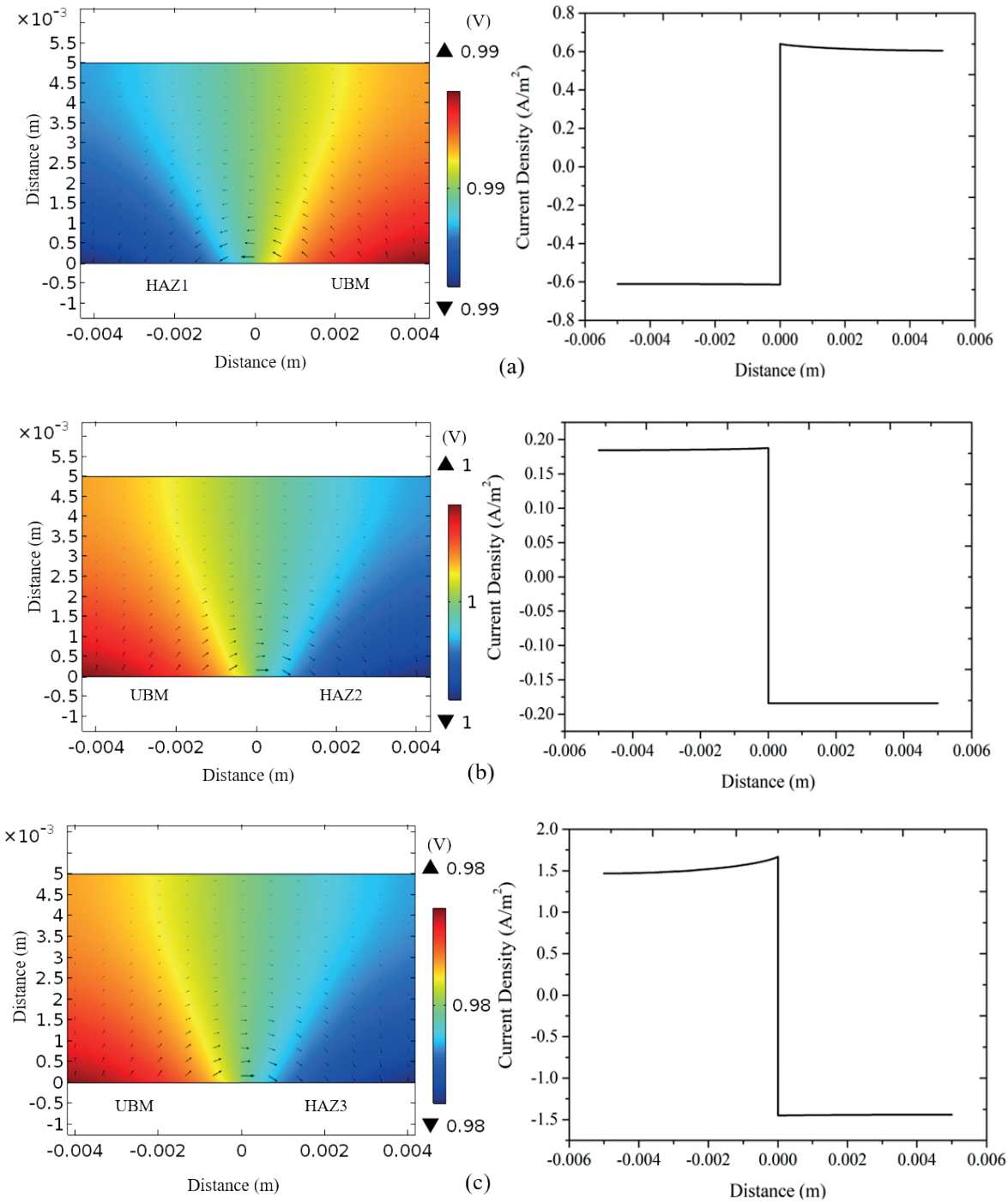

Figure 5: The corrosion potential (left) and corrosion current density (right) predicted using numerical modeling for various galvanic cells in the brazing of galvanized steel, considering various regions (a) region I, (b) region II, (c) region III, (d) region IV, (e) region V, (f) and region VI.

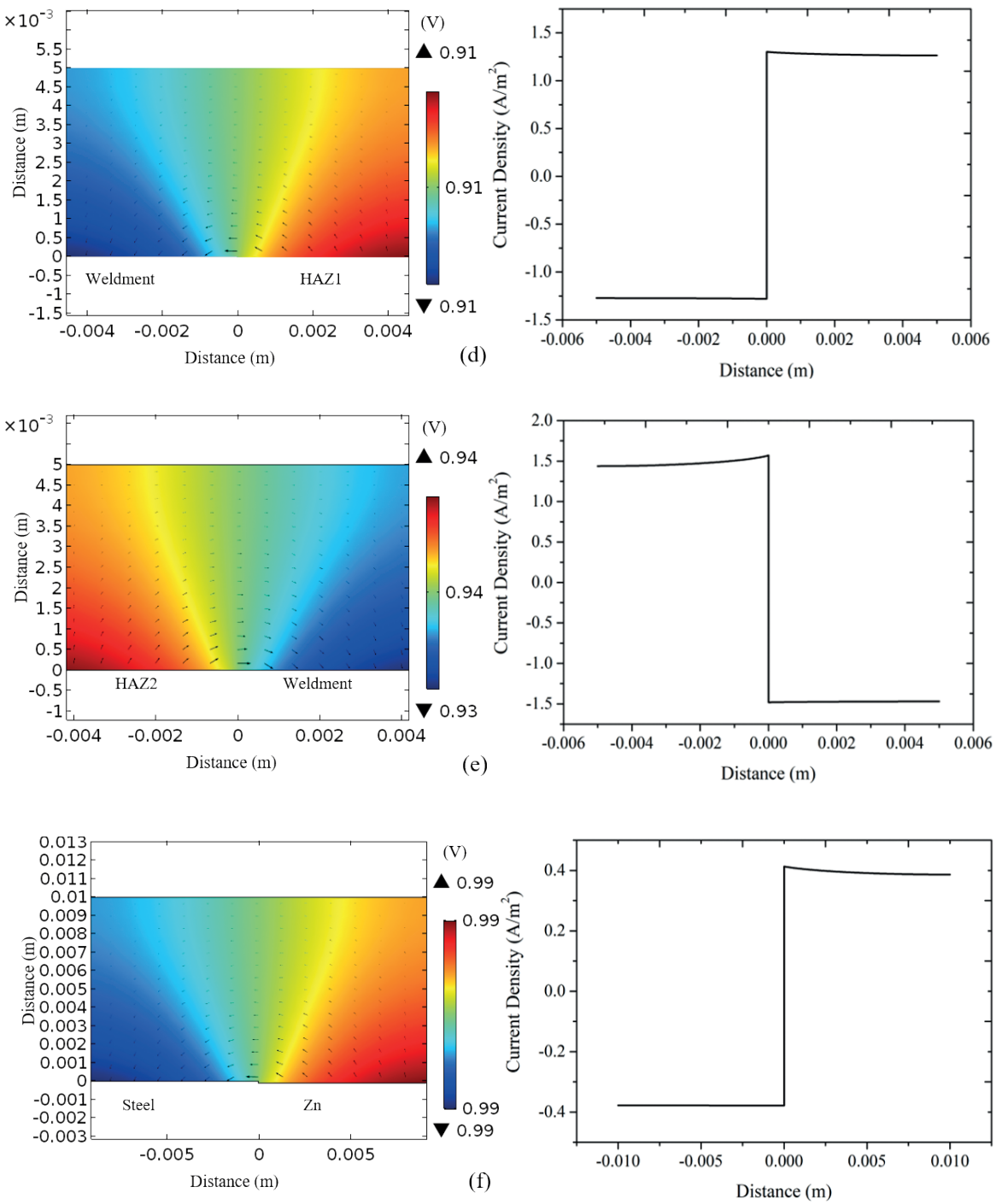

Figure 5: (*Continued*) The corrosion potential (left) and corrosion current density (right) predicted using numerical modeling for various galvanic cells in the brazing of galvanized steel, considering various regions (a) region I, (b) region II, (c) region III, (d) region IV, (e) region V, (f) and region VI.

For the galvanic couples among 1) HAZ1, HAZ2, HAZ3 and the UBM, 2) HAZ1, HAZ2 and the weldment and 3) between steel and the surface, the corrosion current densities obtained from the numerical modeling were similar to that obtained from the mixed potential theory as shown in Table 2.

The corrosion rate was calculated using the mixed potential theory based on Faraday's law in mm/year [8]–[10] (Table 2). Corrosion rates of regions I, II, III, IV, V, VI were 0.853, 0.284, 2.105, 1.754, 2.058, 0.554 mm/y, respectively. Also, the corrosion rate was calculated using the Numerical modeling based on Faraday's law in mm/year (Table 2). Corrosion rates of regions I, II, III, IV, V, VI were 0.913, 0.275, 2.198, 1.904, 2.151, 0.566 mm/y, respectively. The corrosion rates in regions I to VI obtained from the numerical modeling were similar trends to that obtained from the mixed potential theory. However, the corrosion rates obtained from the numerical modeling was higher than that obtained from the mixed potentials theory with the errors less than 8.34%. The corrosion rates from the models were compared with mixed potential theory. In another study, the predicted corrosion rate using the numerical model was 10% of the estimated rate obtained from the mixed potential theory [11]. It was observed that the highest corrosion rate was at regions III, because region III was affected by low heat (Table 2). Also, zinc contents were remained higher in region III than regions I and II [3], [12].

The comparisons of corrosion rates from mixed potentials theory and Numerical modeling were shown in Figure 6. In regions, I, II, III, there were galvanic couple reactions between HAZ and UBM. The result of this couple at HAZ2 had the minimum corrosion rate because HAZ2 was located far from weldment and it was less affected by heat input from the brazing process. HAZ2 has corrosion potential to be similar to UBM and low corrosion rate. In region IV, V, there were galvanic couple reactions between HAZ and weldment. HAZ1 has corrosion potential to be similar to weldment and its corrosion rate was low. Regions VI showed a corrosion rate of galvanized steel [12].

In this study. The corrosion rates obtained from both models were similar. Couple reactions of HAZ and UBM were observed to have the lowest corrosion rates because the HAZ2 was located far away from the heat input that was transmitted by the brazing.

There was a lot of zinc contents remaining on the HAZ2. The corrosion potential difference was therefore close to the surface, causing less corrosion. In a couple of reactions of HAZ and weldment, it was found that region IV had a low corrosion rate. As a result, the corrosion potential difference of HAZ1 was close to the corrosion potentials of the weldment. In a couple of reactions of steel and surface, the corrosion rate of galvanized steel was found to be higher when compared to galvanize steel that has been brazed [12].

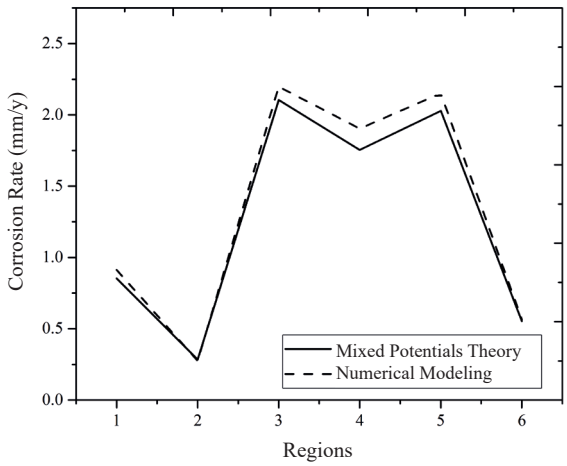

Figure 6: Comparison of corrosion rate from both experimental.

5 Conclusions

Numerical modeling by using COMSOL Multiphysics could predict the corrosion current density (Icorr) among the HAZ and the UBM at HAZ1, HAZ2, and HAZ3. The highest corrosion rate was region III from both experiments because region III was affected by low heat. There was zinc content remained higher than regions I and II. An application of this galvanized steel should be awared, especially at region III. The numerical modeling could also predict corrosion current density among the weldment and the HAZ at HAZ1 and HAZ2. The highest corrosion rate was at region V from both experiments, because region V was affected by high heat. The welding process of galvanized steel should be low heat input at region V. Moreover, it also can predict corrosion current density occured between the surface and steel. The corrosion rate obtained from the mixed potential theory was similar to that obtained from the numerical modeling. The error among the HAZ and the

UBM was less than 10% and among the weldment and the HAZ was less than 10% and between the surface and steel was 10%. The numerical modeling could predict corrosion rate and the result of this work could be used to design the region III during the welding process to had heat input for region V and to maintain zinc thickness in galvanized steel.

References

[1] J. C. Lippold, *Corrosion. In Welding Metallurgy and Weld Ability*. New Jersey: John Wiley & Sons, Inc, 2015, pp. 263–287.

[2] B. N. Popov, *Galvanic Corrosion, Corrosion Engineering*. Amsterdam, Netherlands: Elsevier, 2015, pp. 239–287.

[3] T. Wattanasrisin, "Effects of MIG welding current in brazing process on mechanical properties and microstructure of galvanized steel brazing seam," *The Journal of Industrial Technology*, vol. 12, no. 3, pp. 73–86, Sep. 2016.

[4] A. D. King, J. S. Lee, and J. R. Scully, "Finite element analysis of the galvanic couple current and potential distribution between Mg and 2024-T351 in a Mg rich primer configuration," *Journal of the Electrochemical Society*, vol. 163, no. 7, pp. 342–356, 2016.

[5] F. Cui, F. J. Presuel-Moreno, and R. G. Kelly, "Computational modeling of cathode limitations on localized corrosion of wetted SS 316L at room temperature," *Corrosion Science*, vol. 47, no. 12, pp. 2987–3005, 2005.

[6] E. J. F. Dickinson, H. Ekström, and E. Fontes, "COMSOL Multiphysics®: Finite element software for electrochemical analysis. *A mini-review*," *Electrochemistry Communications*, vol. 40, pp. 71–74, 2014.

[7] L. Y. Xu and Y. F. Cheng, "Development of a finite element model for simulation and prediction of mechano-electrochemical effect of pipeline corrosion," *Corrosion Science*, vol. 73, pp. 150–160, 2013.

[8] K. B. Deshpande, "Validated numerical modelling of galvanic corrosion for couples: Magnesium alloy (AE44)–mild steel and AE44–aluminum alloy (AA6063) in brine solution," *Corrosion Science*, vol. 52, no. 10, pp. 3514–3522, Jul. 2010.

[9] K. B. Deshpande, "Numerical modeling of micro-galvanic corrosion," *Electrochimica Acta*, vol. 56, no. 4, pp. 1737–1745, Sep. 2011.

[10] K. B. Deshpande, "Effect of aluminum spacer on galvanic corrosion between magnesium and mild steel using numerical model and SVET experiments," *Corrosion Science*, vol. 62, pp. 184–191, May 2012.

[11] Y. Lu, H. Jing, Y. Han, and L. Xu, "Numerical modeling of weld joint corrosion," *Journal of Materials Engineering and Performance*, vol. 25, no. 3, pp. 960–965, Jan. 2016.

[12] H. C. Lin, C. A. Hsu, C. S. Lee, T. Y. Kuo, and S. L. Jeng, "Effects of zinc layer thickness on resistance spot welding of galvanized mild steel," *Journal of Materials Processing Technology*, vol. 251, pp. 205–213, 2018.

[13] S. K. Thamida, "Modeling and simulation of galvanic corrosion pit as a moving boundary problem," *Computational Materials Science*, vol. 65, pp. 269–275, 2012.

[14] N. Murer, R. Oltra, B. Vuillemin, and O. Néel, "Numerical modelling of the galvanic coupling in aluminum alloys: A discussion on the application of local probe techniques," *Corrosion Science*, vol. 52, no. 1, pp. 130–139, 2010.

[15] S. R. Cross, S. Gollapudi, and C. A. Schuh, "Validated numerical modeling of galvanic corrosion of zinc and aluminum coatings," *Corrosion Science*, vol. 88, pp. 226–233, 2014.